Chapter 1

Introduction and Review.

1.1 Introduction.

The study of rotating differentially heated fluids is of great importance to the understanding of certain geophysical systems, such as the atmosphere and oceans. The differentially heated, rotating fluid annulus is a system which shares rotational and thermal forcing with these systems, but which has simple, well defined boundary conditions. Since rotating annulus experiments can be run in a laboratory, it is also possible to make a great number and variety of measurements with such a system. While it must be stressed that the rotating annulus is in no sense an engineering model of any particular geophysical system, it is hoped that studies involving the rotating annulus will lead to a greater understanding of the processes taking place in those systems. These studies include both experiments and numerical simulations of the annulus. The relationship between rotating annulus experiments and the atmospheric sciences is illustrated in *Hide (1977)*.

The fact that the flows observed in a differentially heated, rotating annulus bear similarities to larger scale geophysical flows is, in general, unexpected, and arises because the ratios between certain terms in the dynamical equations are similar for flows in the annulus and certain geophysical systems. The interested

reader is referred to *Holton (1979)* (p274), *Hide (1988)*, *Read (1988)* and *White (1988)*.

Interest in rotating annulus systems with barriers is motivated by geophysical systems where zonal flow is obstructed (completely or partially) by topographical features. Examples include the Atlantic Ocean which is bounded by continents and the Antarctic Circumpolar Current as well as the effect of large–scale topography on atmospheric flows.

1.1.1 Motivation.

The work of *Bowden and Eden (1968)* showed that the heat transport through an annulus fully blocked by a radial barrier was far less sensitive to changes in rotation rate than the heat transport through an unblocked annulus.

Hide has suggested (as reported by *Bowden (1961)*) that the fluid heat transport became nearly independent of rotation rate,Ω, because the presence of the barrier allowed an azimuthal pressure gradient to form, so that radial geostrophic flow could advect heat through the fluid. *Bowden and Eden (1968)* found that there was an azimuthal temperature gradient in the fluid, providing evidence to support this view, but did not investigate it systematically. They also observed eddies, which appeared in the system at higher Ω.

The experiments described in this thesis, have attempted to answer the following important questions, which relate to the work above.

1. Is radial geostrophic flow responsible for making the fluid heat transport largely independent of Ω?

2. If radial geostrophic flow cannot maintain the fluid heat transport; or if it can, but only over a limited range of Ω, then what are the processes responsible for keeping the heat transport nearly constant?

3. Do the eddies seen at higher Ω play any significant role in the heat advection of the system, and what causes them?

A second investigation explores the effect of incomplete barriers on the flow. These 'partial barriers' blocked the entire radius of the annulus, but only over a limited height, so that fluid could pass over them. *Kester (1966)* explored the transition from unblocked flow, to flow fully blocked by a barrier. Based on his visual observations, he concluded that there was a relatively sharp transition which occurred when the barrier had a height of about 0.7 times the depth of the annulus. However neither Kester, nor *Leach (1975)* were able to measure any systematic effect on the heat transport through the fluid due to the height of the partial barrier. In Kester's case this was because his heat transport measurements were not sufficiently accurate, while Leach only worked with fairly small barriers, because he was more interested in other aspects of the flow.

Clearly, heat transport measurements are likely to play an important role in understanding the nature of the transition from blocked to unblocked flow, because of the different heat transport characteristics of the unblocked and fully blocked annulus. These characteristics are described in more detail below.

Chapter 7 of this thesis explores the effect of three partial barriers on the flow. The velocity, temperature and heat transport measurements described there lead to a different interpretation of the transition between blocked and unblocked flow in the differentially heated rotating annulus, than that suggested by Kester. However Kester's conclusion is probably correct insofar as it relates to the dependence of the surface flow pattern on the height of his partial barrier.

1.1.2 Acknowledgements.

This thesis brings together work from a variety of sources; this section attempts to indicate what they were.

The apparatus used in the investigations reported in this thesis was provided by the Meteorological Office, initially at Bracknell, and later at the Hooke Institute, Oxford University. The author would like to thank the Director General of the Meteorological Office and the Head of the Hooke Institute for their permission to use it. This thesis is all the author's own work except where stated below.

The author wishes to claim credit for the significant role he played in the reconstruction of the apparatus after it was moved to Oxford, and the long period of time he spent finding and correcting problems caused by the move. He wishes to thank the Hooke Institute technician, Mr Mike Buckler for his invaluable assistance at this time. Thanks are also due to the head of the Hooke Institute, Prof. R.Hide, for the support he was able to provide during the course of this project.

The measurements with the full thermally insulating barrier (chapter 3) were made by Mr.D.W.Johnson, though the author analysed the data. A significant number of the heat and temperature measurements reported in §4.1.2 were also made by Mr.D.W.Johnson, when he was showing the author how to use the apparatus.

The use of sloping bases to suppress the eddies seen in the full barrier experiments and of a thermally conducting barrier was suggested by R.Hide.

The numerical model used in chapter 5, is that of *Hignett et al (1985)*, modified by M.J.Bell and A.A.White to include a radial barrier. The model is mentioned in §1.3.1 and chapter 5. The model was run by Mr.N.Thomas.

1.1.3 Layout of this thesis.

The rest of chapter 1 summarizes the basic theory used in later parts of this thesis (§§1.2.1, 1.2.2), and certain non-dimensional parameters which are found to be helpful in the discussion of rotating fluids. This is followed by a review of previous

related work (§1.3); which is divided into studies involving the unobstructed annulus (§1.3.1), the fully blocked annulus (§1.3.2) and the annulus with partial radial barriers (§1.3.3).

Chapter 2 is divided into two sections, the first is a description of the experimental apparatus used (§2.1) and the second is a discussion of the errors involved in the various types of measurements that were made (§2.2).

Chapters 3,4,6 and 7 deal with the experimental investigations, while chapter 5 covers the investigation with the numerical model mentioned in §1.1.2.

In chapter 3 the results of velocity, temperature and heat transport measurements with a differentially heated, rotating annulus fully blocked by a thermally insulating barrier are presented. The velocity measurements allow certain simplifications to the velocity field to be made, and consequently the fluid heat transport to be related to the azimuthal temperature gradient in the fluid. The results suggest that the fluid heat transport is related to at least two components of the flow (called the η and ζ-circulations in chapter 3) and possibly a third (the eddies seen at higher rotation rates). A mechanism for one of these (the η-circulation) is proposed in §3.2.3, and tested in §3.2.4.

An attempt to critically test the mechanism for the η-circulation is made in chapter 4. This was done by trying to modify the azimuthal temperature gradient in the fluid by using a thermally conducting barrier in place of the insulating barrier of chapter 3. While the azimuthal temperature gradient proved remarkably resilient to such a change, the results raise certain questions about how the fluid manages to support the temperature difference observed across the barrier.

In chapter 5 a computer simulation of the flow has been used to attempt to identify the mechanism for the ζ-circulation mentioned above. A mechanism is proposed in §5.4.1 and tested in §5.4.2. The model seems to demonstrate that the

mechanism suggested in §5.4.1 is inappropriate. §5.4.3 proposes an alternative mechanism for the ζ-circulation and the model is used to provide evidence which supports it.

Chapter 6 explores the role of the eddies observed in the experiments reported in chapter 3. Sloping bases have been found to suppress the formation of baroclinic waves in an unobstructed annulus flow (see §1.3.1 and chapter 6). If a sloping base can be used to suppress the eddies observed in the annulus with a fully blocking thermally insulating barrier, then by comparison with the results of chapter 3, it may be possible to draw conclusions about the heat transport properties, and even the nature of the eddies observed in the system. One of the bases used in chapter 6 did suppress the formation of the eddies over the whole range of Ω used (at a certain externally applied temperature difference). The results obtained also provided additional evidence to support the mechanism advanced for the η-circulation in §3.2.3.

In chapter 7 a slightly different series of investigations are reported. These explore the transition from fully blocked to unblocked flow in the differentially heated rotating annulus, by using barriers of finite azimuthal width with heights of two-thirds and one-third of the depth of the annulus. The flow in the presence of the two-thirds barrier appeared to have certain features in common with the fully blocked system. This result was used to obtain estimates of the heat transport in the regions above and below the top of the barrier. The results seem to suggest that the advective heat transport in such a system is, to a fairly good approximation, given by a linear combination of the heat advection of a fully blocked and unblocked system based on the height of the barrier.

The conclusions from the combined investigations of chapters 3 to 6, as well as a summary of the conclusions of chapter 7 are given in chapter 8.

A list of symbols and their definitions is given before chapter 1.

1.2 Theoretical considerations.

1.2.1 The equation of motion.

Laboratory experiments have centred around work on incompressible, electrically insulating, fluids. Only Newtonian fluids, where ν is independent of $\vec{u}$ (see below for the definitions of ν and $\vec{u}$) are considered. The equation of motion for such a fluid in a rotating system is (see e.g. *Tritton (1988)*),

$$\frac{\partial \vec{u}}{\partial t} + (\vec{u}.\nabla)\vec{u} + 2\vec{\Omega} \times \vec{u} = -\frac{1}{\rho}\nabla p + \nabla\Phi + \nu\nabla^2\vec{u}, \tag{1.1}$$

where $\vec{u}$ is the velocity of a fluid element, $\vec{\Omega}$ is the angular velocity of the system, ρ is the mass density of the fluid, p is the pressure, ν is the assumed constant kinematic viscosity of the fluid, and Φ the potential of external forces. In cylindrical polar coordinates (r, ϕ, z), $\nabla\Phi = \vec{g} - \vec{\Omega} \times (\vec{\Omega} \times \vec{r}) + \vec{F}_{ext}$, where $\vec{g} = -g\hat{z}$ is the acceleration due to gravity, and $\vec{F}_{ext}$ represents the acceleration due to any other external forces.

The equation of conservation of mass for a fluid is

$$\frac{\partial \rho}{\partial t} + \nabla.(\rho\vec{u}) = \frac{\partial \rho}{\partial t} + (\vec{u}.\nabla)\rho + \rho\nabla.\vec{u} = 0.$$

As stated above, only incompressible fluids are considered, so that ρ is constant following the motion of a fluid particle, and,

$$\frac{D\rho}{Dt} \equiv \frac{\partial \rho}{\partial t} + (\vec{u}.\nabla)\rho = 0.$$

So the mass continuity equation becomes

$$\nabla.\vec{u} = 0. \tag{1.2}$$

If the fluid density is linearly dependent on temperature T, the density of the incompressible fluid is given by

$$\rho = \bar{\rho}[1 - \alpha(T - \bar{T})]. \tag{1.3}$$

Here $\bar{\rho}$ is the density of the fluid at the mean fluid temperature $\bar{T}$, and α is the coefficient of thermal expansion for the fluid.

The conductive heat flux vector for a fluid is $\vec{H}_{cond} = -k\nabla T$ $(W.m^{-2})$, where k is the thermal conductivity of the fluid. The advective heat flux vector is

$$\vec{H}_{adv} = \rho C_p \vec{u} T \ (W.m^{-2}), \tag{1.4}$$

where C_p is the specific heat capacity of the fluid. So that the equation of conservation of heat is

$$\frac{\partial}{\partial t}(\rho C_p T) + \nabla.(\vec{H}_{cond} + \vec{H}_{adv}) = 0.$$

For an incompressible (1.2), Boussinessq fluid (so that in this case ρ may be regarded as a constant), this reduces to the equation of heat transfer

$$\frac{\partial T}{\partial t} + \vec{u}.\nabla T = \kappa\nabla^2 T + Q. \tag{1.5}$$

Here $\kappa = k/\rho C_p$ is the thermometric conductivity of the fluid and is assumed to be constant. Q represents the possibility of internal heat sources in the fluid. In the experiments described in this thesis there are no such sources, hence $Q = 0$.

Equations (1.1) $\rightsquigarrow$ (1.3) and (1.5) form a set of six equations in six unknowns, $\vec{u}, p, \rho, T$.

To express buoyancy effects explicitly the density may be split into a mean density, $\bar{\rho}$ and the assumed small fluctuations from it, ρ', so that $\rho = \bar{\rho} + \rho'$. By reference to equation (1.3) it can be seen that $\rho' = -\bar{\rho}\alpha(T - \bar{T})$. Hence $\rho\nabla\Phi = \bar{\rho}\nabla\Phi + \rho'\nabla\Phi$ and

$$\nabla\Phi = \frac{\bar{\rho}}{\rho}\nabla\Phi + \frac{\rho'}{\rho}\nabla\Phi.$$

So that by assuming that $\rho' \approx 0$ except when it is coupled with gravity, and that $\rho \approx \bar{\rho}$ equation (1.1) can be expressed in terms of the Boussinesq approximation

$$\frac{\partial \vec{u}}{\partial t} + (\vec{u}.\nabla)\vec{u} + 2\vec{\Omega} \times \vec{u} = -\frac{1}{\bar{\rho}}\nabla p + \nabla\Phi - \alpha(T - \bar{T})\nabla\Phi + \nu\nabla^2\vec{u}. \tag{1.6}$$

A further simplification can be made by assuming that the main contribution to $\nabla\Phi$ comes from gravity, *i.e.* $|\Omega^2 r| \ll |g|$. If ΔT is a good estimate of the typical value of $(T - \bar{T})$, then the magnitude of buoyancy forces can be estimated as $|g\alpha\Delta T|$.

1.2.2 Scaling the equation of motion.

At this point it is useful to scale equation (1.6) for fluid motions appropriate to rotating annulus experiments to gain some idea of the physical processes likely to be important in that system.

To do this the horizontal and vertical components of the motions were scaled separately and the results used to derive the 'thermal wind' equation. The scaling was performed using typical data from the experiments using the annulus described in chapter 2.

Typical horizontal velocities were seen to be of order $U \sim 10^{-4}\ m.sec^{-1}$, and the horizontal length scale used was $L \sim (b - a)$ in the radial direction, and $\pi(a + b)$ in the azimuthal direction. Ω varied between 0 and 5.0 $rad.sec^{-1}$ so $\Omega \sim 1\ rad.sec^{-1}$ was used. Horizontal pressure variations present a potential problem as they were not measured, however the results of a computer model by *Hignett et al. (1985)* suggest that horizontal deviations in $p/\bar{\rho}$ can be estimated as $\sim 10^{-4}\ m^2.sec^{-2}$. Steady state motions only are considered. The scaling analyses for the horizonal components of the equation of motion are given in *Table 1.1.*

Component from term	Scale of term	Magnitude of term
$(\vec{u}.\nabla)\vec{u}$	$\frac{U^2}{L}$	$10^{-7}\ m.sec^{-2}$
$2\vec{\Omega} \times \vec{u}$	$2\Omega U$	$10^{-4}\ m.sec^{-2}$
$\frac{1}{\bar{\rho}}\nabla p$	$\frac{\Delta p}{\bar{\rho}L}$	$\sim 10^{-3}\ m.sec^{-2}$
$\nu\nabla^2\vec{u}$	$\nu\frac{U}{L^2}$	$10^{-7}\ m.sec^{-2}$

TABLE 1.1(a): Scaling analysis for the radial equation of motion.

Component from term	Scale of term	Magnitude of term
$(\vec{u}.\nabla)\vec{u}$	$\frac{U^2}{L}$	$10^{-8}\ m.sec^{-2}$
$2\vec{\Omega} \times \vec{u}$	$2\Omega U$	$10^{-4}\ m.sec^{-2}$
$\frac{1}{\bar{\rho}}\nabla p$	$\frac{\Delta p}{\bar{\rho}L}$	$\sim 10^{-4}\ m.sec^{-2}$
$\nu\nabla^2\vec{u}$	$\nu\frac{U}{L^2}$	$10^{-7}\ m.sec^{-2}$

TABLE 1.1(b): Scaling analysis for the azimuthal equation of motion.

Thus the primary balance that must occur on surfaces of constant potential, Φ is between the Coriolis and pressure gradient forces, this is known as 'geostrophic balance'. It holds to an accuracy $\sim 10^{-7}/10^{-4} = 0.1\%$ by comparison with the magnitude of the next largest term.

The experiments did not measure vertical velocities in the annulus, however typical values for the vertical velocities have been estimated by *Jackson and Hignett (1984)* as $w \sim 10^{-5}\ m.sec^{-1}$. The vertical length scale used was d (see chapter 2), so that $\nabla \sim d^{-1} \sim 7\ m^{-1}$. Vertical pressure differences were estimated as $\Delta p \sim \rho g d$, and buoyancy forces as $g\alpha\Delta T \sim 10^{-2}\ m.s^{-2}$. The scaling analysis for the vertical equation of motion is given in *Table 1.2.*

Component from term	Scale of term	Magnitude of Term
$(\vec{u}.\nabla)\vec{u}$	$\frac{W^2}{d}$	$10^{-9}\ m.sec^{-2}$
$\frac{1}{\bar{\rho}}\nabla p$	$\frac{\Delta p}{\rho d}$	$10\ m.sec^{-2}$
$\nabla\Phi$	g	$10\ m.sec^{-2}$
$\alpha(T - \bar{T})\nabla\Phi$	$g\alpha\Delta T$	$10^{-2}\ m.sec^{-2}$
$\nu\nabla^2\vec{u}$	$\nu\frac{W}{L^2}$	$10^{-8}\ m.sec^{-2}$

TABLE 1.2: Scaling analysis for the vertical equation of motion.

So it can be seen that the primary balance occurs between the vertical pressure gradient forces and gravity, this is known as 'hydrostatic balance', and it holds $\sim 10^{-2}/10 = 0.1\%$ by comparing it with the next largest term.

The results of the scaling analysis performed above can be used to derive the so–called thermal wind equation. In cylindrical polar coordinates (r, ϕ, z), with velocity, $\vec{u} = (u, v, w)$, geostrophic balance can be expressed,

$$2\Omega v \approx \frac{1}{\bar{\rho}}\frac{\partial p}{\partial r}, \quad \text{and} \tag{1.7}$$

$$2\Omega u \approx -\frac{1}{r\bar{\rho}}\frac{\partial p}{\partial \phi}, \tag{1.8}$$

while hydrostatic balance was:

$$\frac{1}{\bar{\rho}}\frac{\partial p}{\partial z} \approx -g + \alpha g(T - \bar{T}). \tag{1.9}$$

So that by taking $\partial/\partial z$ of equations (1.7) and (1.8), and $\partial/\partial r$ or $\partial/\partial\phi$ of (1.9) p can be eliminated to give;

$$\frac{\partial v}{\partial z} \approx \frac{g\alpha}{2\Omega}\frac{\partial T}{\partial r}, \quad \text{and} \tag{1.10}$$

$$\frac{\partial u}{\partial z} \approx -\frac{g\alpha}{2\Omega r}\frac{\partial T}{\partial \phi}, \tag{1.11}$$

the two components of the thermal wind equation. Since these have been derived using geostrophy and hydrostatic balance (which were each expected to be correct to $\sim 0.1\%$ for flow in the interior of the fluid) so the thermal wind equation may be expected to be accurate to about 0.1% in similar circumstances.

1.2.3 Dimensionless parameters.

It is useful to define certain non-dimensional parameters which are helpful in the discussion of rotating fluids. Because these parameters are based on the ratios of various terms in equations (1.1) and (1.5) their magnitude helps to indicate which physical processes are important in determining the flow in the system.

The Rossby number, Ro is the ratio of the inertial acceleration $|(\vec{u}.\nabla)\vec{u}| \sim U^2/L$ to the Coriolis acceleration $|2\vec{\Omega} \times \vec{u}| \sim 2\Omega U$ in the system,

$$\mathrm{Ro} = \frac{U}{2\Omega L}. \tag{1.12}$$

The Taylor number τ compares the square of viscous processes $|\nu\nabla^2\vec{u}| \sim \nu U/L^2$ to the square of the Coriolis acceleration,

$$\tau = \frac{4\Omega^2 L^4}{\nu^2}. \tag{1.13}$$

The Rayleigh number compares the ratio of buoyancy forces and viscous effects in equation (1.6) with advective and conductive heat transport processes in equation (1.5).

$$\mathrm{Ra} = \frac{g\alpha\Delta T L^3}{\nu\kappa} = \mathrm{Gr.Pr}, \tag{1.14}$$

where Gr is the Grashof number and Pr the Prandtl number, mentioned below. The Grashof number is Gr= $g\alpha\Delta T L^3/\nu^2$. For large Grashof number, it is the square of the magnitude of the buoyancy force $|g\alpha(T - \bar{T})|$, divided by the square of the magnitude of the viscous force $|\nu\nabla^2\vec{u}|$, where the typical fluid velocity is estimated from an inertial ($|\vec{u}.\nabla\vec{u}|$) buoyancy balance. Thus Gr$\gg$ 1 indicates that the inertia and buoyancy forces are much more important than the viscous forces in the fluid. The same interpretation does not apply to small Gr, since then the balance between inertial and buoyancy forces may not be valid. For further details see *Tritton (1988)* pages 172-174. The Ekman number Ek compares viscous and Coriolis effects,

$$\mathrm{Ek} = \frac{\nu}{2\Omega L^2}. \tag{1.15}$$

Another important ratio is given by the Prandtl number, Pr which by comparing the viscous and thermal diffusivities is assumed to remain a constant for the fluid.

$$\mathrm{Pr} = \frac{\nu}{\kappa}. \tag{1.16}$$

The Nusselt number is a dimensionless measure of the heat advection through the fluid, and compares the total heat transport through the fluid with the conductive heat transport, thus

$$\mathrm{Nu} = \frac{H_{adv} + H_{cond}}{H_{cond}}. \tag{1.17}$$

So that when all the heat transport through the fluid is due to conduction, Nu=1.

1.3 Review of previous work.

1.3.1 The unobstructed annulus.

The first attempts to use experiments to examine flow in rotating fluids were qualitative in nature. The work of Vettin from 1857–1884, Exner in 1923 and others is reviewed by *Fultz (1951)* and *Fultz et al. (1959)*. *Thomson (1892)* had also suggested the use of a differentially heated rotating tank to investigate the motions of the atmosphere. In the light of later discoveries it seems that Vettin observed axisymmetric flow in his experiments, while Exner saw irregular flow. *Fowlis (1964)* reviews this early work in some detail.

A significant contribution was made by *Hide (1953) (a), (b), (1958)*, who carried out experiments on thermal convection in a rotating cylindrical annulus. By careful control of the experimental conditions Hide was able to establish the importance of a non-dimensional parameter, Θ which he expressed as

$$\Theta = \frac{gd}{\frac{1}{2}\Omega^2(b^2 - a^2)} \frac{\Delta\rho}{\rho} \frac{1}{2} \frac{(b+a)}{(b-a)}.$$

He found that for an unobstructed annulus two fundamentally different types of flow occurred depending on whether Θ was greater, or less than

$\Theta_{crit} = 1.58 \pm 0.05$. For $\Theta > \Theta_{crit}$ the flow was axially symmetric, while for $\Theta < \Theta_{crit}$ a regular (baroclinic) [1] wave flow was observed. By use of equation (1.3) Θ can be re-expressed to give,

$$\Theta \equiv \frac{g\alpha\Delta T d}{\Omega^2(b-a)^2}. \tag{1.18}$$

Θ is a Rossby number (1.12) where U is based on the linearized thermal wind equation (1.10). Hide also observed two other types of flow, both associated with high values of Ω; irregular flow, and wave vacillation.

Davies (1956) showed that barotropic theory was unable to explain the transition for the onset of regular waves seen by Hide, and that approximate baroclinic theory gave results that appeared to be in reasonable agreement, so far as his analysis went. *Robinson (1959)* theoretically investigated the axisymmetric regime of flow and was able to show that flow in the main body of the fluid was governed by the geostrophic thermal wind. He also collated the experimental results of several authors to produce a qualitative diagram of the regimes of flow as a function of Θ and τ (the earliest such diagram seen by this author).

Heat transport measurements for an unobstructed annulus were made by *Bowden (1961)*. He found that for a stationary annulus the heat transport was given by

$$\mathrm{Nu}(\Omega = 0) = (0.203 \pm 0.010)(\mathrm{Pr.Gr})^{\frac{1}{4}}. \tag{1.19}$$

He also performed a few preliminary experiments with a fully blocking radial barrier.

Fowlis and Hide (1965) confirmed the importance of Θ (which they called Π_4) they also demonstrated that axisymmetric flow occurred for all values of Θ when the parameter $\Pi_5 < (1.85 \pm 0.08) \times 10^5$. Where Π_5 was defined,

[1] The regular wave flow was not shown to be baroclinic in nature until a later date.

$\Pi_5 \equiv 4\Omega^2(b-a)^5/\nu^2 d$. Reference to equation (1.13) shows that Π_5 is identical to τ when the characteristic length scale L, is defined so that $L^4 \equiv (b-a)^5/d$. This is used to define the Taylor number,

$$\tau \equiv \frac{4\Omega^2(b-a)^5}{\nu^2 d}. \tag{1.20}$$

Notice that Θ and τ are external parameters to the system because they are defined in terms including quantities external to the fluid $(a, b, d, \Omega, \Delta T)$ rather than using characteristic length scales generated by fluid motions, for example, or temperature differences within the fluid. *Figure 1.1* shows a so-called 'regime diagram' similar to the one *Fowlis and Hide (1965)* obtained. They were also able to show that *Eady's* treatment of baroclinic instability *(1949)* in an inviscid fluid was able to predict the approximate value that Θ tended to in the limit $\tau \to \infty$, suggesting that the regular wave regime was a manifestation of baroclinic instability.

Bowden and Eden (1965) examined the fluid velocity and temperature fields and heat transport in the axisymmetric regime, with and without a rigid lid at the upper surface. They found that the heat transport was less with an upper free surface, and that there was a discontinuity in the heat transport between the axisymmetric and regular wave regimes. They also observed the azimuthal velocity, v, and found that it was approximately in agreement with the linearized thermal wind equation, with $v = 0$ close to mid-depth (with a rigid upper lid).

By considering the flow through the Ekman layers that form on the lid and base of the annulus, *Hide (1967)(a), (b)* was able to obtain an expression for the heat transport in the axisymmetric flow regime, which fell off with rotation rate as approximately $\Omega^{-3/2}$. This result is also described in *Hide and Mason (1975)*. Further, by calculating the average vertical temperature contrast, *Hide (1967) (b)* was able to show that there was very close agreement between

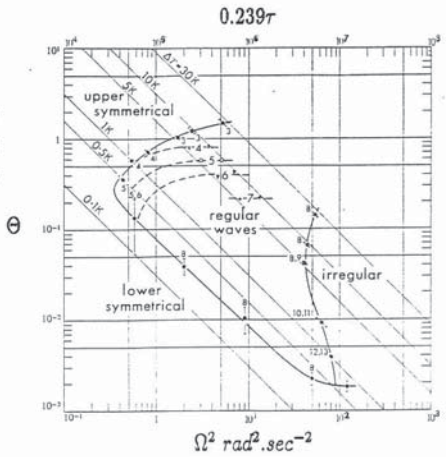

FIGURE 1.1: Typical regime diagram illustrating the dependence of the mode of convection on Θ and τ. From *Hide and Mason (1975)*.

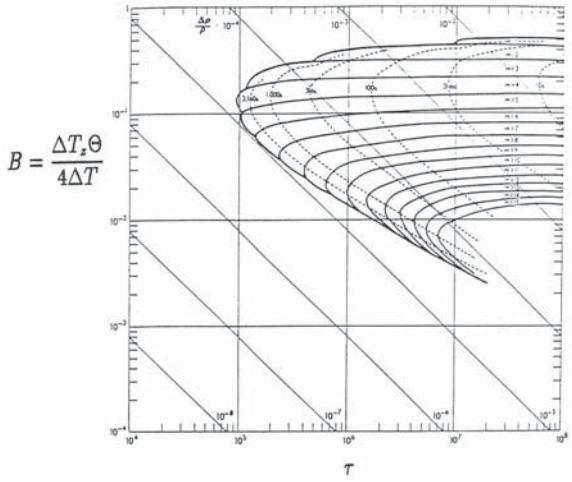

FIGURE 1.2: Regime diagram based on the theory of baroclinic instability taking into account Ekman–layer friction at rigid upper and lower horizontal surfaces. The full lines denote the transition from axisymmetric to non–axisymmetric flow, or from non–axisymmetric flow of one wavenumber (m) to another wavenumber. B is an internal dimensionless parameter for the fluid, which may be regarded as $B = \Delta T_z \Theta/(4\Delta T)$, where ΔT_z is an appropriate vertical temperature difference in the fluid. From *Hide and Mason (1975)*.

the transition for the onset of regular waves in the annulus in the experiments in the limit $\tau \to \infty$, and inviscid baroclinic instability theory.

Hide (1969) extended the theory of baroclinic instability to include the effects of Ekman layer suction. He found that his theory predicted stable flow for $\tau < \tau_{crit}$ in addition to the condition on Θ predicted by the inviscid theory. He estimated the value of τ_{crit} and found that it agreed reasonably with experimental measurements.

Mason (1972), (1975) explored the effect of sloping bases on the baroclinic wave flows seen in the unobstructed annulus, following theoretical work by *Hide (1969)*. He found that at sufficiently high rotation rates, fluid particles felt the presence of a sloping base throughout the depth of the fluid. He was thus able to use sloping bases to cause fluid particles to move at certain angles to the geopotentials in the fluid, with the effect of suppressing or assisting sloping convection (depending on the sense and steepness of the slope). This work is also discussed in *Hide and Mason (1975)*. The effect of sloping bases is discussed in chapter 6.

Hide and Mason (1975) reviews the work with the rotating annulus, including such phenomena as the various types of wave vacillation which are not discussed here, and includes an example of a regime diagram calculated from *Hide's (1969)* theory, *Figure 1.2*. Hide also included the effects of sloping boundaries.

Hide (1977) summarizes much of the theory associated with the rotating annulus work, he also discusses the experimental work, *Figure 1.3* shows heat transport measurements in various annulus systems from *Hide (1977)*, including those with a fully blocking radial barrier (see also §1.3.2).

Since then attention has shifted towards detailed examination of several of the flows observed in the annulus, such as the characteristics of the baroclinic waves, (*Hide, Mason and Plumb (1977)*) and using a numerical model of the flow, *James, Jonas and Farnell (1981)*. *Hignett et al. (1985)* used a numerical

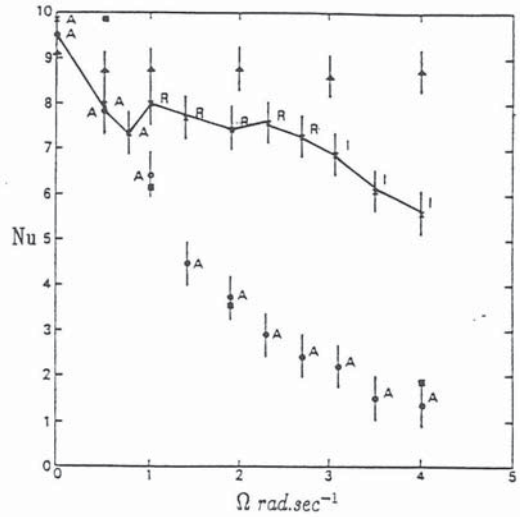

FIGURE 1.3: Plot showing the dependence of Nu on Ω for thermal convection in a typical differentially heated rotating fluid annulus. Nu=1 corresponds to purely conductive heat transfer. Key: 'A' denotes axisymmetric flow, 'R' regular baroclinic waves, and 'I' irregular baroclinic waves. The crosses and solid line show results from an unobstructed system with horizontal end walls, the circles show results with sloping end walls which suppressed non–axisymmetric flow (see *Hide and Mason (1975)*), and the triangles show results from a system fully blocked by a rigid barrier. The squares are based on a simple theoretical model of heat transfer due to axisymmetric flow (*Hide (1967)(a), (b)*). Taken from *Hide (1977)*.

model to qualitatively simulate various features observed in the experimental flows, including wavenumber transitions, amplitude vacillation and weak shape vacillation.

Further reviews and comparisons with processes occuring in atmospheric flows are given in *Hide (1985), (1986), (1988), Read (1988)*. The numerical simulations of rotating annulus flows are discussed in *Hignett et al. (1985)* and *White (1988)*.

A recent theoretical contribution was made by *Hide (1989)* who suggested

that the average value of a quantity P over the fluid would be expected to be zero under certain circumstances, where $P \equiv (\nabla \times \vec{u}).\nabla \ln \rho$. This would provide an additional equation to describe the flow.

1.3.2 The annulus with a fully blocking radial barrier.

Rotation greatly reduces heat advection through the fluid in an unblocked annulus. *Bowden (1961)* (§8.2), reports Hide's suggestion that a thin radial barrier, that completely blocked the annulus cavity at one value of ϕ, might enable an azimuthal temperature and pressure gradient to form, resulting in radial geostrophic flow. If this was the case, it was to be expected that a full radial barrier might annul, either in part, or completely, the effects of rotation on heat transfer through the system. However Bowden's work was inconclusive.

An investigation of the fully blocking radial barrier system was made by *Bless (1965)* in his Bachelor's thesis, under the direction of R.Hide. He made no heat transport measurements, but did observe three regimes of flow, which were; (i) flow parallel to the inner and outer cylinders at small rotation rates and temperature contrasts, (ii) vortex cells at high Ω and ΔT, and (iii) an intermediate regime.

Hide (1968) suggested that a fully blocking radial barrier could influence the main body of the fluid, so that it would be unaffected by rotation.

Bowden and Eden (1968) made heat transport measurements in a similar system, and found that the heat transport diminished far less with rotation rate in the presence of a full radial barrier, than in an unblocked system. They also made measurements of fluid temperature and found that the full barrier modified the isotherms, so that the radial temperature gradient was much reduced compared with an unblocked system. *Figure 1.4* shows diagrams of fluid isotherms against radius in fully blocked systems. They found that the fluid temperature had a

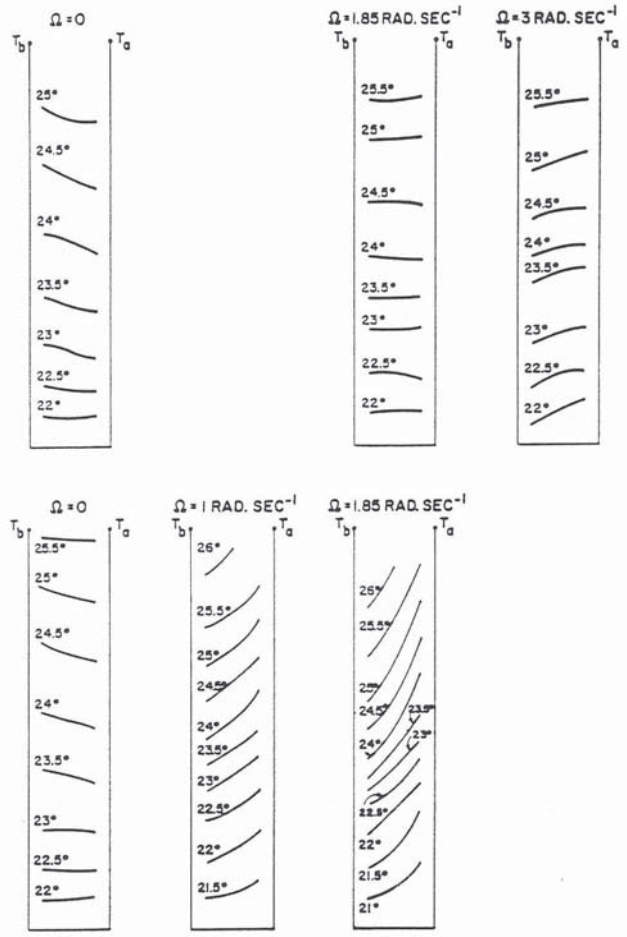

FIGURE 1.4(a): Experimental measurements of fluid temperature against height and radius over a range of Ω with $\Delta T \approx 6\ K$. Upper results are for an annulus with a full radial barrier, lower results are for an unblocked annulus. In both cases $a = 3\ cm$, $b = 5\ cm$, $T_b = 26°C$, $T_a = 20°C$ and $d = 10\ cm$. In the fully blocked annulus $\partial T/\partial r$ is much smaller than in the unblocked annulus. From *Bowden and Eden (1968)*.

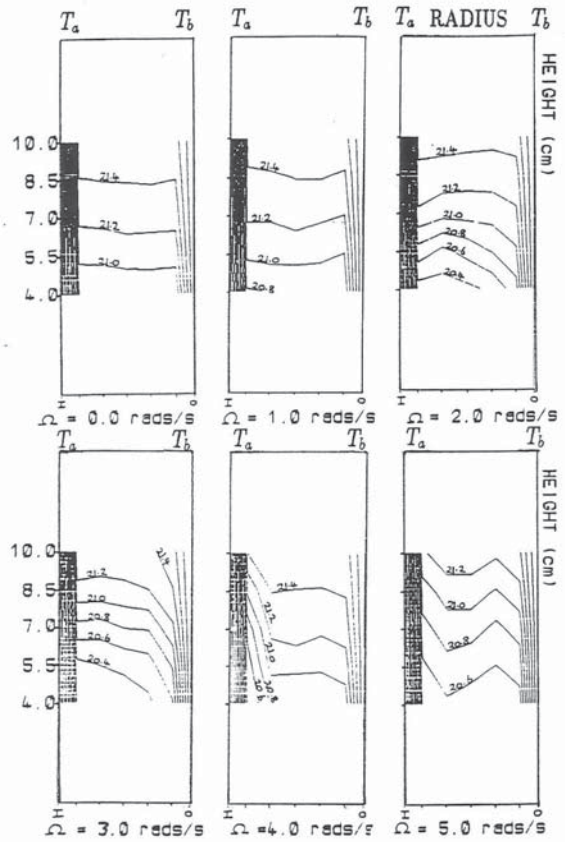

FIGURE 1.4(b): Experimental measurements of fluid temperature against height and radius over a range of Ω with $\Delta T \approx 4\ K$, for an annulus fully blocked by a thermally insulating barrier. In most cases $\partial T/\partial r$ is small in the interior of the fluid. Results provided by D.W.Johnson (private communication).

fairly smooth dependence on ϕ at low Ω, which became jagged at high Ω. They suggested that the heat transport in the full radial barrier system was due to a radial geostrophic flow which was supported by an azimuthal pressure gradient, so that a radial cell developed, rather like that seen in a stationary annulus. However without systematic measurements of the azimuthal temperature gradient they were unable to test this idea.

Experiments with a rotating, differentially heated, rectangular tank were made by *Condie and Griffiths (1989)*. While such a system is not a fully blocked rotating annulus, it is topologically similar to the blocked annulus, being singly connected. They investigated the steady flow and observed a horizontal cyclonic circulation when the cooled wall was near the axis of rotation. By noticing the effect of a sloping base on this horizontal circulation they were able to show that it was caused by centrifugal effects. Their conclusions are discussed in chapter 5.

The numerical model used by *Hignett et al. (1985)* was modified by M.J.Bell and A.A.White to include a full insulating radial barrier (A.A.White, private communication). This model is used to explore an aspect of the flow in chapter 5.

1.3.3 The annulus with partial radial barriers.

This review is restricted to work involving rotating flow over obstacles which are roughly similar to the partial barriers mentioned in §2.1.1 and chapter 7. This is necessary because while there is a vast literature on topographic effects, there is comparatively little published material on the sorts of systems investigated in this thesis.

Of particular relevance is the work of *Kester (1966)*, who, for his Bachelor's thesis, investigated annulus flows in the presence of thin barriers, which blocked the entire radius, but only the lower part of the cavity. By examining the sur-

face flow pattern, he found a relatively abrupt transition, between blocked and unblocked flow, when the barrier had a height of $0.7d$ (d being the depth of the annulus cavity). Unfortunately, Kester did not calibrate his instruments before use, so it is perhaps not surprising that his heat transport measurements found no difference between the heat transports without any barrier, and with a fully blocking barrier. His work is discussed in chapter 7.

Fultz and Spence (1967) used ridges with an azimuthal width of 60° and a triangular cross–section, as well as thin barriers. Their barriers had a maximum height of about $0.4d$. By observing the surface flow patterns, they found that the waves they saw in the system were distorted as they passed over the ridges.

Boyer (1970), (1971) looked at homogeneous rotating flow over a long shallow ridge for a fluid with $\mathrm{Ek} \ll 1$. For background rotation in the same sense as the northern hemisphere he found that down stream of the step, the streamlines were shifted to the right.

Leach (1975) studied various types of topography in a differentially heated rotating annulus. His 'type C' topography was very similar to one of the partial barriers described in this thesis, and the results he obtained with it are discussed elsewhere, as appropriate. In his theoretical work, Leach fitted a topographic bottom boundary to a baroclinic basic flow. He states that the waves seen with his topography types were free baroclinic waves. The waves tended to play a reduced role in the transport of heat in the system, which Leach attributed to the heat transport of the topographically forced wave. As well as working with end wall topography he also investigated the flow in an eccentric annulus.

The steady flow of a homogeneous, incompressible fluid in a rotating annulus with shallow topography (of trapezoidal cross–section) was investigated by *Davey (1978)* using a numerical model. The flow was driven by a differentially rotating lid. He obtained results for three regimes, which depended on the relative sizes of

Ek and Ro. A linear viscous regime ($\mathrm{Ek}^{1/2} \gg \mathrm{Ro}$), an inviscid regime ($\mathrm{Ek}^{1/2} \ll \mathrm{Ro}$) and an intermediate regime ($\mathrm{Ek}^{1/2} \sim \mathrm{Ro}$). Examples of his results are given in *Figure 1.5.* He extended his investigation to include steady rotating flow over topography in a β–plane channel in *Davey (1980)* and a β–plane annulus in *Davey (1981).*

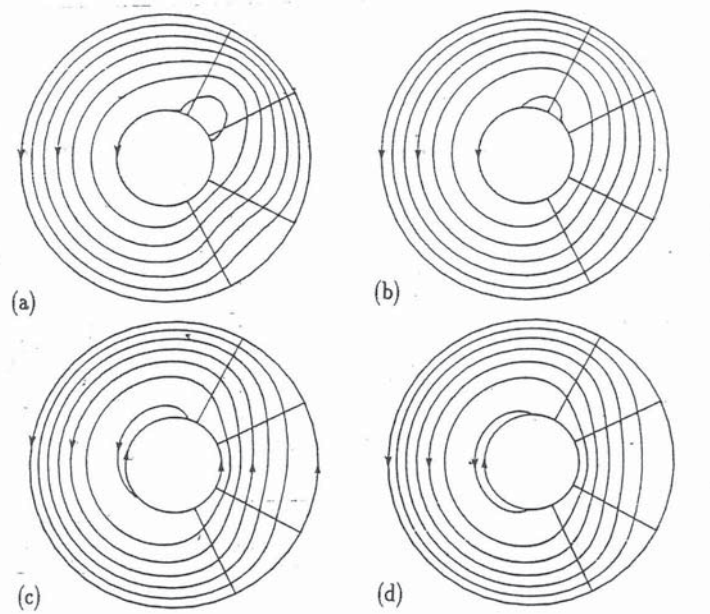

FIGURE 1.5: Streamlines showing simulated flow over small trapezoidal cross–section topography in a rotating annulus. The flow is forced by a differentially rotating lid. (a) Linear viscous flow, $\mathrm{Ek}^{1/2} = 0.1$, $\mathrm{Ro} \to 0$. (b) Intermediate flow, $\mathrm{Ek}^{1/2} = 0.1$, Ro=0.1. (c) Inviscid flow, $\mathrm{Ek}^{1/2} = 0.01$, Ro=0.1. (d) Inviscid flow, $\mathrm{Ek}^{1/2} \to 0$, Ro=0.1. From *Davey (1978).*